# Enhanced thermoelectric performance in Bi-doped p-type AgSbTe2 compounds

Rajeshkumar Mohanraman, Raman Sankar, F. C. Chou, C. H. Lee, and Yang-Yuan Chen

Citation: Journal of Applied Physics **114**, 163712 (2013); doi: 10.1063/1.4828478
View online: http://dx.doi.org/10.1063/1.4828478
View Table of Contents: http://scitation.aip.org/content/aip/journal/jap/114/16?ver=pdfcov
Published by the AIP Publishing

# Enhanced thermoelectric performance in Bi-doped p-type $AgSbTe_2$ compounds

Rajeshkumar Mohanraman,[1,2,3,a)] Raman Sankar,[4] F. C. Chou,[4,5,6] C. H. Lee,[1,5] and Yang-Yuan Chen[2,7,a)]
[1]*Department of Engineering and System Science, National Tsing Hua University, Hsinchu, Taiwan*
[2]*Institute of Physics, Academia Sinica, Taipei, Taiwan*
[3]*Nano Science and Technology, Taiwan International Graduate Program, Academia Sinica, Taipei, Taiwan*
[4]*Center for Condensed Matter Sciences, National Taiwan University, Taipei, Taiwan*
[5]*National Synchrotron Radiation Research Center, Hsinchu, Taiwan*
[6]*Center for Emerging Material and Advanced Devices, National Taiwan University, Taipei, Taiwan*
[7]*Graduate Institute of Applied Physics, National Chengchi University, Taipei, Taiwan*

(Received 20 May 2013; accepted 16 October 2013; published online 31 October 2013)

The influence of bismuth (Bi) substitution on the thermoelectric properties of $AgSbTe_2$ compounds was investigated and compared with the undoped $AgSbTe_2$. The addition of Bi dopants not only resulted in a reduction in thermal conductivity but also markedly increased the thermopower in the $Ag(Sb_{1-x}Bi_x)Te_2$ series. Additional phonon scatterings were created by Bi doping and led to a reduction of thermal conductivity. The lattice thermal conductivity is significantly reduced which could be ascribed to enhancement of phonon scattering by dopants with greater atomic weight. In addition, the thermopower was enhanced, which was attributed to the electron-filtering effects caused by the nanoscaled microstructures. Because of the extremely low thermal conductivity ($0.48\ Wm^{-1}K^{-1}$) and moderate power factor of $AgBi_{0.05}Sb_{0.95}Te_2$, a maximum ZT value of ($1.04 \pm 0.08$) was reached at 570 K; yielding an enhancement of greater than 10% compared with an undoped $AgSbTe_2$. this result shows promising thermoelectric properties in the medium temperature range. © *2013 AIP Publishing LLC*. [http://dx.doi.org/10.1063/1.4828478]

## I. INTRODUCTION

Energy and the environment have become critical issues in the 21st century. The urgent need for sources of energy other than fossil fuels, as well as the most efficient use of current fossil-fuel supply, has prompted urgent research into alternative energy sources and various types of energy conversion technologies. One type of energy conversion technology that has gained renewed attention is thermoelectric (TE) energy conversion, where heat is converted directly into electricity using a class of materials known as thermoelectric materials.[1–7] TE materials are becoming increasingly important in the field of electricity generation and environmentally friendly refrigeration devices.[1,2] The performance of TE devices is assessed using the dimensionless figure of merit $ZT = \alpha^2\sigma T/\kappa$, where $\alpha$, $\sigma$, T, and $\kappa$ are the Seebeck coefficient, the electrical conductivity, the absolute temperature, and the thermal conductivity, respectively. Based on the above relationship, the optimally performing TE materials should possess high electrical conductivity, a large Seebeck coefficient, and low thermal conductivity.[1]

$AgSbTe_2$ has been firmly established as a potential thermoelectric material[8–16] because of its relatively low thermal conductivity ($0.6–0.7\ Wm^{-1}K^{-1}$).[17,18] $AgSbTe_2$ is widely identified as a disordered NaCl type (Fm-3 m) where Ag and Sb randomly occupy the Na site.[19] According to previous studies,[16] the disordered lattice structure dominantly contributes to low lattice thermal conductivity through Umklapp and intrinsic phonon-phonon scattering processes without substantial reduction in electrical conductivity. Recently, the $AgSbTe_2$ compound has attracted considerable attention in constructing so-called bulk nanostructured TE materials, such as $(AgSbTe_2)_{1-x}(PbTe)_x$ (LAST) and $(AgSbTe_2)_{1-x}(GeTe)_x$ (TAGS) with excellent TE properties.[20–25]

Doping is a potential approach to optimize the thermoelectric properties of p-type $AgSbTe_2$ by reducing its thermal conductivity and adjusting its carrier concentration. In this study, trivalent $Bi^{3+}$ ions were selected to substitute $Sb^{3+}$ ions in a p-type $Ag(Sb_{1-x}Bi_x)Te_2$ system to dramatically suppress lattice thermal conductivity while simultaneously contributing to the thermopower enhancement.

The BiTe-$AgSbTe_2$ solid solution has been studied.[26] It is interesting that the transport properties of $(AgSbTe_2)(BiTe)_x$ were reported only for the $x = 0.01$ composition.[26] In the present work, we investigated the role of higher concentration of Bi substitution on the thermoelectric properties of $Ag(Sb_{1-x}Bi_x)Te_2$ series at 300 K to 600 K. We found that when $x = 0.05$, the sample exhibited a maximum ZT value of ZT value of ($1.04 \pm 0.08$) at 570 K, and is therefore a potential candidate for use as a p-type TE material. Thus, the influence of Bi-doping on the thermodynamic properties, microstructure, and TE transport behavior in $Ag(Sb_{1-x}Bi_x)Te_2$ (i.e., $x > 0$, designated as Bi-AST) samples is systematically investigated in this study.

[a)]Authors to whom correspondence should be addressed. Electronic addresses: rajeshx@phys.sinica.edu.tw. Tel.: 886-2-2817-5274 and cheny2@phys.sinica.edu.tw. Tel.: 886-2-2789-6725. Fax: 886-2-2783-4187.

 

## II. EXPERIMENTAL

High-purity starting elements of Ag (99.999%, shot), Sb (99.9999%, shot), Bi (99.999%, chunks), and Te (99.999%, shot) were weighed according to the stoichiometric ratio of $Ag(Sb_{1-x}Bi_x)Te_2$ ($x = 0$, 0.03, 0.05, 0.07, and 0.1) and then sealed into carbon-coated quartz tubes with a diameter of 13 mm under high vacuum ($10^{-3}$ Torr). The quartz tube was heated at 1073 K for 10 h (including rocking to facilitate complete mixing and homogeneity of the liquid phase) and then cooled to 773 K over 6 days and finally followed by cooling to room temperature over 10 h. Highly dense single phase ingots with a dark silvery metallic shine were obtained. These ingots were stable in water and air. The obtained crystalline ingots were cut and polished into approximately $3 \times 3 \times 12\,mm^3$ rectangular shapes, and circular discs with 12 mm diameters and thicknesses 1–2 mm for later physical property measurements. The density of the ingots measured using the Archimedes method varied from 7.11 to 7.12 $g/cm^3$, which is greater than 99.9% of the theoretical density.

X-ray diffraction (XRD) experiments were conducted for phase identifications by using a powder X-ray diffractometer (X'Pert PRO-PANalytical, CuK$\alpha$ radiation) at $2\theta$ angles of 20°–80°. With these data, the lattice parameters of $Ag(Sb_{1-x}Bi_x)Te_2$ ($x = 0$, 0.03, 0.05, 0.07, and 0.1) samples were calculated using the Rietveld refinement program. Fractured surface morphology was characterized using field emission scanning electron microscopy (FESEM, Hitachi, S-4800). The chemical composition of the as-prepared ingots was determined using wavelength dispersive X-ray fluorescence spectrometry (WD-XRF). The Hall effect was measured at room temperature under 0.55 T with a four probe configuration using the van der Pauw method (ECOPIA HMS-5000). The electrical conductivity $\sigma$ and the Seebeck coefficient $\alpha$ were measured simultaneously using commercial equipment (ZEM-3, ULVAC-RIKO, Japan) in a He atmosphere from 300 to 600 K. The thermal conductivity $\kappa$ was calculated using the equation $\kappa = D\ C_p\ d$ from the thermal diffusivity $D$ obtained using a laser flash apparatus (NETZSCH, LFA 457), specific heat $C_p$ was determined by using a differential scanning calorimeter (NETZSCH, STA 449), and the density $d$ was obtained using the Archimedes method. Uncertainties in the $\sigma$, $\alpha$, and $\kappa$ are $\pm 2\%$, $\pm 2\%$, and $\pm 3\%$, respectively, leading to about maximum 8% uncertainty in ZT.

## III. RESULTS AND DISCUSSION

### A. Structural analysis

Crystalline ingots of $Ag(Sb_{1-x}Bi_x)Te_2$ were cut and polished for the transport-property measurements. Fig. 1 presents powder XRD patterns of samples with the composition $Ag(Sb_{1-x}Bi_x)Te_2$, where $x = 0$, 0.03, 0.05, 0.07, and 0.1. All diffraction peaks can be indexed into the face-centered cubic (FCC) $AgSbTe_2$ structure (reference code: 01-089-3671) without any indication of secondary phase impurities. The lattice parameter as a function of the Bi fraction is displayed in the inset of Fig. 1. As can be seen,

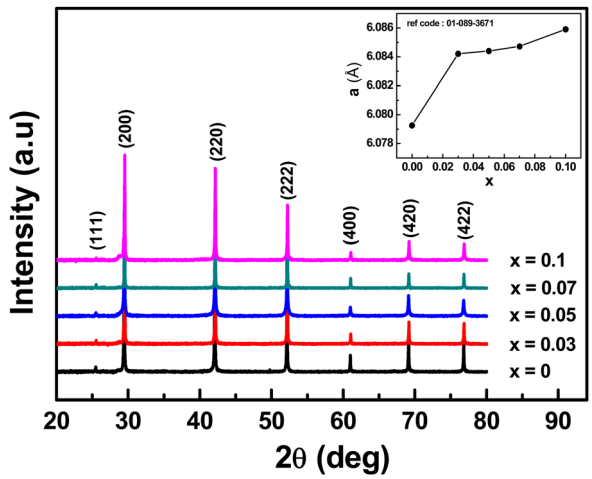


FIG. 1. Powder XRD patterns of $Ag(Sb_{1-x}Bi_x)Te_2$ ($x = 0$, 0.03, 0.05, 0.07, and 0.1) samples. The inset shows the Bi content (x) composition dependence of lattice parameter (a) fitted by Rietveld method.

the substitution of Sb atoms (atomic radius ~140 pm) with bigger Bi atoms (atomic radius ~156 pm) leads to an increase of the lattice parameter. Fig. 2 shows the FESEM image of the free-fracture surface of the $AgBi_{0.05}Sb_{0.95}Te_2$ sample. The magnified image (in the inset of Fig. 2) shows a highly compact structure, which is in agreement with the density measurements.

The composition variation of the $Ag(Sb_{1-x}Bi_x)Te_2$ series obtained from wavelength dispersive X-ray fluorescence analysis were in good agreement with those of the nominal compositions (Table I).

### B. Thermoelectric properties

The temperature dependence of the electrical conductivity $\sigma$ measured in the range of 300 to 600 K is shown in Fig. 3(a). For all Bi-AST samples, the electrical conductivity decreased with increasing temperature for $T < 500$ K and then slightly increased at $T > 500$ K, indicating the semi-conducting transport behavior. The Bi-AST samples showed lower $\sigma$ compared with the undoped $AgSbTe_2$ compound at room temperature (Table I) due to the decrease in the carrier concentration. Table I shows the properties used to describe the electron

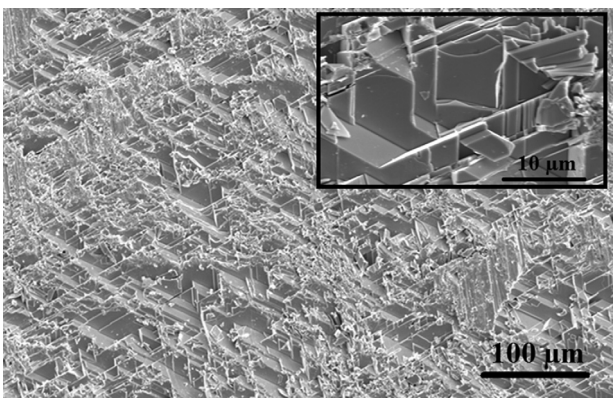


FIG. 2. SEM image of the bulk $AgBi_{0.05}Sb_{0.95}Te_2$. The inset shows a magnified portion.

TABLE I. Physical properties of $Ag(Sb_{1-x}Bi_x)Te_2$ compounds at room temperature (carrier concentration $N$, Hall mobility $\mu_H$, electrical conductivity $\sigma$, Seebeck coefficient $\alpha$, effective mass $m^*/m_o$ and XRF composition of $Ag(Sb_{1-x}Bi_x)Te_2$ (x = 0, 0.03, 0.05, 0.07, and 0.1) samples).

| Nominal composition | XRF composition | $N$ ($10^{19}$ cm$^{-3}$) | $\mu_H$ (cm$^2$V$^{-1}$s$^{-1}$) | $\sigma$ ($10^4$ Sm$^{-1}$) | $\alpha$ ($\mu$VK$^{-1}$) | $m^*/m_o$ |
|---|---|---|---|---|---|---|
| $AgSbTe_2$ | $Ag_{0.98}Sb_{1.016}Te_2$ | 13.8 | 16.2 | 3.6 | 164 | 2.08 |
| $AgBi_{0.03}Sb_{0.97}Te_2$ | $AgBi_{0.024}Sb_{0.982}Te_2$ | 2.32 | 29.4 | 1.10 | 244 | 1.0 |
| $AgBi_{0.05}Sb_{0.95}Te_2$ | $AgBi_{0.043}Sb_{0.967}Te_2$ | 7.2 | 17.47 | 2.02 | 201 | 1.73 |
| $AgBi_{0.07}Sb_{0.93}Te_2$ | $AgBi_{0.067}Sb_{0.918}Te_2$ | 3.7 | 21.1 | 1.26 | 222 | 1.24 |
| $AgBi_{0.1}Sb_{0.9}Te_2$ | $AgBi_{0.089}Sb_{0.83}Te_2$ | 1.68 | 32 | 0.85 | 172 | 0.9 |

transport characteristics of Bi-doped $Ag(Sb_{1-x}Bi_x)Te_2$ compounds at room temperature. Compared with the undoped $AgSbTe_2$, the Bi-AST samples displayed a lower carrier concentration but higher mobility.

The Seebeck coefficients of all the specimens were positive, as shown in Fig. 3(b), indicating p-type conduction. At room temperature, the Seebeck coefficient $\alpha$ for Bi-AST samples ranged from 172 to 244 $\mu$VK$^{-1}$ is higher than that of the undoped $AgSbTe_2$ sample. The Seebeck coefficient for metals or degenerate semiconductors, with the assumption of a parabolic band and energy independent scattering, can be expressed as[27,31]

$$\alpha = \frac{8\pi^2 k B^2 T}{3qh^2} m^* \left(\frac{\pi}{3n}\right)^{\frac{2}{3}}, \quad (1)$$

where $n$ is the carrier concentration, $k_B$ is Boltzmann constant, $q$ is the electronic charge, $h$ is the Planck constant, and $m^*$ is the effective mass. The effective masses were calculated with Eq. (1) and listed in Table I. In this work, the maximum Seebeck coefficient value of 244 $\mu$VK$^{-1}$ were obtained for the sample (x = 0.03) with minimum effective mass value of 1.0 $m_0$ at room temperature. So, we cannot suggest that the increase of the effective mass is the reason for the increase of the Seebeck coefficient. The possible reason for the increase in the Seebeck coefficient may be connected to the electron filtering effects caused by the nanoscaled microstructures.[11,28,31] The power factor P.F = $\alpha^2\sigma$ curves were plotted in Fig. 3(c). The power factor initially increased, reached a maximum, and then decreased when the temperature increased. The power factor for undoped $AgSbTe_2$ sample had the largest values over the full temperature range, whereas Bi-AST samples had lower power factor except sample with x = 0.05 had achieved moderate value.

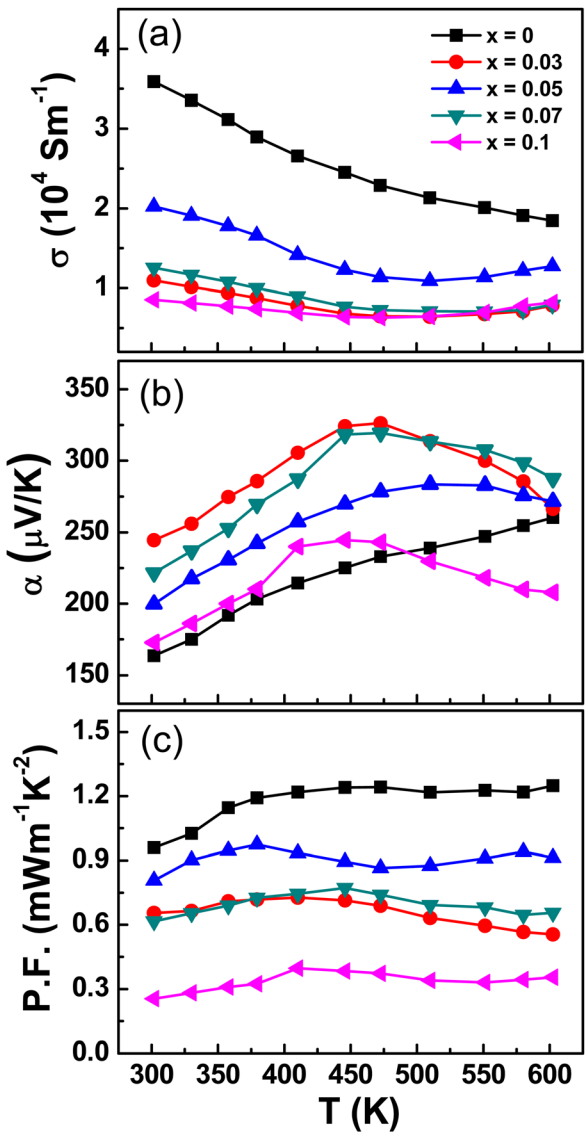


FIG. 3. Temperature dependence of (a) electrical conductivity, (b) Seebeck coefficient, and (c) power factor of $Ag(Sb_{1-x}Bi_x)Te_2$ (x = 0, 0.03, 0.05, 0.07, and 0.1) samples.

Fig. 4(a) shows the temperature dependence of the thermal diffusivity $D$ and measured specific heat capacity $Cp$ of $Ag(Sb_{1-x}Bi_x)Te_2$ samples. Based on the specific heat data, the results closely match the literature value ($Cp \sim 0.205$ Jg$^{-1}$K$^{-1}$) of $AgSbTe_2$.[17] Total thermal conductivity is calculated as a product of the measured specific heat at constant pressure $Cp$, thermal diffusivity $D$, and mass density $d$. Fig. 4(b) shows the temperature dependence of the total thermal conductivity of the $Ag(Sb_{1-x}Bi_x)Te_2$ samples. For all samples, the $\kappa$ first decreased and subsequently increased when the temperature increased, and the magnitude spanned from 0.48 to 0.91 Wm$^{-1}$K$^{-1}$. The thermal conductivity of the sample with x = 0.05 exhibited the lowest thermal conductivity in the temperature range of 300–600 K with a minimum of 0.48 Wm$^{-1}$K$^{-1}$ at 510 K. At temperatures higher than 550 K, the thermal conductivity gradually increases, due to the occurrence of ambipolar contribution, which is more significant at higher temperature.[29] Since the total thermal conductivity has two components, it can be expressed as $\kappa = \kappa_e + \kappa_L$, where the electronic thermal conductivity ($\kappa_e$) is attributed to carriers (electrons and holes), and the lattice thermal conductivity ($\kappa_L$) is related to phonons. For the

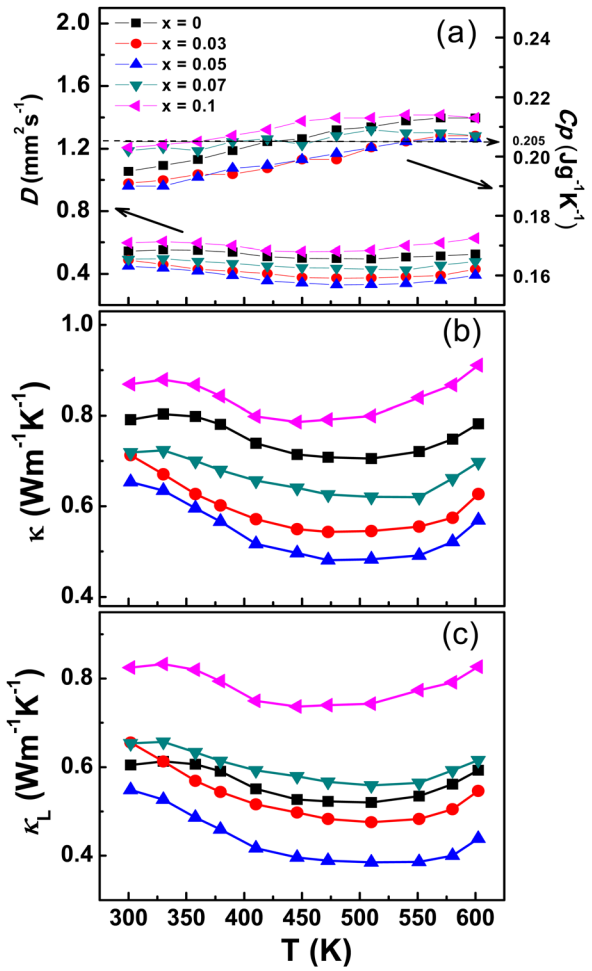


FIG. 4. Temperature dependence of (a) diffusivity and specific heat capacity, (b) total thermal conductivity, and (c) lattice thermal conductivity of $Ag(Sb_{1-x}Bi_x)Te_2$ (x = 0, 0.03, 0.05, 0.07, and 0.1) samples.

Bi-AST, the lattice term ($\kappa_L$), which is obtained by subtracting the electrical contributor ($\kappa_e$) from $\kappa$, contributes more than 90% of the total thermal conductivity ($\kappa$), in other words the ambipolar contribution can be neglected. The electrical contribution, $\kappa_e$, is estimated from the Wiedemann–Franz law, $\kappa_e = L\sigma T$, where $L = 0.7L_0$ (Ref. 16) ($L_0$ is the Lorenz factor for free electrons with a value of $2.45 \times 10^{-8}$ $V^2K^{-2}$). This calculation reveals that the heat is conducted mainly by lattice phonons, and the electronic contribution is less than 10% of total thermal conductivity. As shown in Fig. 4(c), the sample with $x = 0.05$ exhibited a lower lattice thermal conductivity ($0.38\,Wm^{-1}K^{-1}$) than undoped $AgSbTe_2$ ($0.52\,Wm^{-1}K^{-1}$) at 510 K, close to the minimal theoretical thermal conductivity ($0.3\,Wm^{-1}K^{-1}$) reported by Cahill *et al.*[30] With Bi doping, the electronic contribution to the thermal conductivity is decreased due to the decrease of electrical conductivity. As shown in Fig. 4(c), the lattice thermal conductivity decreases with increasing Bi content for $x \leq 0.05$ because of the enhancement of phonons scattering; however, when x increased further, the lattice thermal conductivity increases when $x \geq 0.07$, indicating $x = 0.05$ is the optimal doping. Further in-depth studies are needed to gain better understanding for higher concentration. Isoelectronic substitution introduces mass fluctuation scattering and strain field fluctuation scattering for phonons due to the mass and size differences between alloying atoms and host atoms.[32–36] In other words, here in our work (Bi doped $AgSbTe_2$), while replacing Sb site by heavier atom Bi atoms in $Ag(Sb_{1-x}Bi_x)Te_2$ system creates enhanced effective phonon scatterings by the highly disordered Ag/Sb lattice. This result shows that isoelectronic substitution of Bi for Sb is an effective way to reduce the lattice thermal conductivity in $AgSbTe_2$ system.

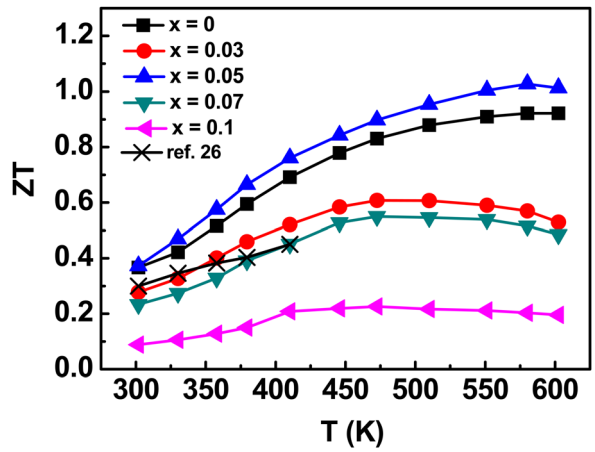


FIG. 5. Temperature dependence of thermoelectric figure of merit ZT of $Ag(Sb_{1-x}Bi_x)Te_2$ (x = 0, 0.03, 0.05, 0.07, and 0.1) samples.

The TE figure of merit ZT was calculated from the measured values of $\sigma$, $\alpha$, and $\kappa$ by using the equation $ZT = \alpha^2\sigma T/\kappa$. Fig. 5 shows the temperature dependence of the ZT of all $Ag(Sb_{1-x}Bi_x)Te_2$ (x = 0, 0.03, 0.05, 0.07, and 0.1) compounds. The highest ZT value was observed in $AgBi_{0.05}Sb_{0.95}Te_2$, which reached $(1.04 \pm 0.08)$ at 570 K. This value is 10% higher than that of the undoped $AgSbTe_2$ at the same temperature. In addition, for $AgBi_{0.05}Sb_{0.95}Te_2$ sample, we achieved a ZT value 70% higher than that reported for $(BiTe)_{x=0.01}(AgSbTe_2)$[26] at 400 K. These results show a marked improvement in the TE figure of merit ZT for Bi-doped AST samples.

## IV. CONCLUSION

We investigated the TE properties of Bi-doped $Ag(Sb_{1-x}Bi_x)Te_2$ compounds. XRD analysis indicated that single-phase material crystallizes in a cubic NaCl-type structure in Bi-doped $AgSbTe_2$ samples. The Seebeck coefficient increased and the electrical conductivity decreased with increasing Bi doping. The thermal conductivity was markedly reduced with Bi doping. The lattice thermal conductivity reduction was primarily responsible for the overall decrease in thermal conductivity. The lattice contribution had a larger effect on the total thermal conductivity than the electronic contribution at all the examined temperatures. This result was because of the additional phonon scatterings, which were created by Bi doping. A maximum ZT value of $(1.04 \pm 0.08)$ was obtained for the sample $AgBi_{0.05}Sb_{0.95}Te_2$ at 570 K, which is 10% higher than that of undoped AgSbTe2, showing promising thermoelectric properties in the medium-temperature range.

## ACKNOWLEDGMENTS

This work was supported by Academia Sinica and the National Science Council, Taiwan, Republic of China, Grant No. NSC100-2112-M-001-019-MY3.

[1]D. M. Rowe, *Thermoelectrics Handbook: Macro to Nano* (CRC, Boca Raton, FL, 2006), Chap. 1.
[2]G. S. Nolas, J. Sharp, and J. Goldsmid, *Thermoelectrics: Basic Principles and New Materials Developments* (Springer, New York, 2001).
[3]T. M. Tritt and M. A. Subramanian, *Thermoelectric Materials, Phenomena, and Applications: A Birds Eye View* (MRS Bull., 2006), Vol. 31, p. 188.
[4]L. E. Bell, Science **321**, 1457 (2008).
[5]G. Chen, M. S. Dresselhaus, G. Dresselhaus, J. P. Fleurial, and T. Caillat, Int. Mater. Rev. **48**, 45 (2003).
[6]M. S. Dresselhaus, G. Chen, M. Y. Tang, R. G. Yang, H. Lee, D. Z. Wang, Z. F. Ren, J. P. Fleurial, and P. Gogna, Adv. Mater. **19**, 1043 (2007).
[7]J. Yang and F. Stabler, J. Electron. Mater. **38**, 1245 (2009).
[8]S. N. Zhang, T. J. Zhu, S. H. Yang, C. Yu, and X. B. Zhao, Acta Mater. **58**, 4160 (2010).
[9]H. Wang, J. F. Li, M. Zhou, and T. Sui, Appl. Phys. Lett. **93**, 202106 (2008).
[10]J. Xu, H. Li, B. Du, X. Tang, Q. Zhang, and C. Uher, J. Mater. Chem. **20**, 6138 (2010).
[11]S. N. Zhang, T. J. Zhu, S. H. Yang, C. Yu, and X. B. Zhao, J. Alloys Compd. **499**, 215 (2010).
[12]J. D. Sugar and D. L. Medlin, J. Alloys Compd. **478**, 75 (2009).
[13]H. A. Ma, T. C. Su, P. W. Zhu, J. G. Guo, and X. P. Jia, J. Alloys Compd. **454**, 415 (2008).
[14]D. L. Medlin and J. D. Sugar, Scr. Mater. **62**, 379 (2010).
[15]P. A. Sharma, J. D Sugar, and D. L. Medlin, J. Appl. Phys. **107**, 113716 (2010).
[16]B. Du, H. Li, J. Xu, X. Tang, and C. Uher, Chem. Mater. **22**, 5521 (2010).
[17]D. T. Morelli, V. Jovovic, and J. P. Heremans, Phys. Rev. Lett. **101**, 035901 (2008).
[18]E. F. Hockings, Phys. Chem. Solids **10**, 341 (1959).
[19]R. W. Armstrong, J. W. Faust, and W. A. Tiller, J. Appl. Phys. **31**, 1954 (1960).
[20]K. F. Hsu, S. Loo, F. Guo, W. Chen, J. S. Dyck, C. Uher, T. P. Hogan, E. K. Polychroniadis, and M. G. Kanatzidis, Science **303**, 818 (2004).
[21]X. Z. Ke, C. F. Chen, J. H. Yang, L. J. Wu, J. Zhou, Q. Li, Y. M. Zhu, and P. R. C. Kent, Phys. Rev. Lett. **103**, 145502 (2009).
[22]W. Q. Ao, W. A. Sun, J. Q. Li, F. S. Liu, and Y. Du, J. Alloys Compd. **475**, L22 (2009).
[23]H. Wang, J. F. Li, C. W. Nan, M. Zhou, W. S. Liu, B. P. Zhang, and T. Kita, Appl. Phys. Lett. **88**, 092104 (2006).
[24]B. A. Cook, M. J. Kramer, X. Wei, J. L. Harringa, and E. M. Levin, J. Appl. Phys. **101**, 053715 (2007).
[25]J. R. Salvador, J. Yang, X. Shi, H. Wang, and A. A. Wereszczak, J. Solid State Chem. **182**, 2088 (2009).
[26]V. Jovovic and J. P. Heremans, J. Electron. Mater. **38**, 1504 (2009).
[27]M. Cutler, J. F. Leavy, and R. L. Fitzpatrick, Phys. Rev. **133**, A1143 (1964).
[28]J. M. O. Zide, D. Vashaee, Z. X. Bian, G. Zeng, J. E. Bowers, A. Shakouri, and A. C. Gossard, Phys. Rev. B **74**, 205335 (2006).
[29]V. Jovovic and J. P. Heremans, Phys. Rev. B **77**, 245204 (2008).
[30]D. G. Cahill, S. K. Watson, and R. O. Pohl, Phys. Rev. B **46**, 6131–6140 (1992).
[31]B. K. Min, B. S. Kim, I. H. Kim, J. K. Lee, M. H. Kim, M. W. Oh, S. D. Park, and H. W. Lee, Electron. Mater. Lett. **7**, 255–260 (2011).
[32]B. Abeles, Phys. Rev. **131**, 1906 (1963).
[33]P. G. Klemens, Phys. Rev. **119**, 507–509 (1960).
[34]J. Callaway and H. C. von Baeyer, Phys. Rev. **120**, 1149–1154 (1960).
[35]L. Zhou, W. Li, J. Jiang, T. Zhang, Y. Li, G. Xu, and P. Ci, J. Alloys Compd. **503**, 464–467 (2010).
[36]S. R. Boona and D. T. Morelli, Appl. Phys. Lett. **101**, 101909 (2012).